Long-term Expression of Apolipoprotein B mRNA-specific Hammerhead Ribozyme via scAAV8.2 Vector Inhibits Atherosclerosis in Mice

Hersharan Nischal[1], Hua Sun[1,2], Yuchun Wang[1,5], David A Ford[4], Ying Cao[3], Peng Wei[3] and Ba-Bie Teng[1,2]

Target substrate-specific hammerhead ribozyme cleaves the specific mRNA efficiently and results in the inhibition of gene expression. In humans, overproduction of apolipoprotein B (apoB) is positively associated with premature coronary artery diseases. The goal of this study is to demonstrate that long-term reduction of apoB gene expression using hammerhead ribozyme would result in inhibition of atherosclerosis development. We designed two hammerhead ribozymes targeted at the nucleotides of apoB mRNA GUC^{2326} (designated RB1) and GUA^{6679} (designated RB15), and we used self-complementary adeno-associated virus 8.2 (scAAV8.2) vector to deliver these active ribozymes of RB1, RB15, combination of RB1/RB15, and an inactive hammerhead ribozyme RB15 mutant to atherosclerosis-prone LDb mice (_Ldlr$^{-/-}$Apobec1$^{-/-}$_). LDb mice lack both low density lipoproteins (LDL) receptor (_Ldlr$^{-/-}$_) and apoB mRNA editing enzyme (_Apobec1$^{-/-}$_) genes and develop atherosclerosis spontaneously. After the RB1, RB15, or combination of RB1/RB15 ribozymes treatment, the LDb mice had significantly decreased plasma triglyceride and apoB levels, resulting in markedly decreased of atherosclerotic lesions, Furthermore, the active ribozymes treatment decreased the levels of diacylglycerol acyltransferase 1 (Dgat1) mRNA and the levels of multiple diacylglycerol (DAG) molecular species. These results provide the first evidence that decreased apoB levels results to reduction of Dgat1 expression and triglyceride levels (TAG), which had a significant impact on the development of atherosclerosis.

Introduction

Hammerhead ribozyme belongs to a family of small catalytic RNAs capable of doing an endonucleolytic self-cleavage reaction.[1] Uhlenbeck[2] and Haseloff and Gerlach[3] engineered substrate-specific hammerhead ribozymes that efficiently cleave target substrate RNAs in _trans_. This discovery has led to the development of many substrate-specific hammerhead ribozymes to downregulate gene expression _in vitro_ and _in vivo_. Ribozymes emerged as an important RNA based therapeutic approaches; they have been used to manipulate cellular gene expressions in many disease models ranging from inhibition of HIV activity to cancer therapy.[4] The approaches of ribozymes are challenged by the discovery of siRNAs, because it is relatively difficult to identify the effective ribozyme target sites compared with siRNA. However, ribozymes exhibit less off-target effects as found in RNA interference mechanisms.[5] Thus, the recent ribozyme library approach may prove to be an effective way to identify an appropriate target site on the mRNA[6] to develop the RNA inhibition therapeutic approach.

Our laboratory has designed and engineered hammerhead ribozyme that cleaves apolipoprotein B (apoB) mRNA at GUA^{6679} efficiently, and we designated it as RB15.[7,8] RB15 was delivered to cells[8] and mice[7] via adenoviral vector. It has been shown to cleave apoB mRNA at the specific target site

efficiently, resulting in a marked decrease in plasma cholesterol, triglyceride, and apoB, when compared with the inactive ribozyme RB15 mutant. These results indicated that apoB mRNA-specific hammerhead ribozyme could be used as a potential therapeutic agent to modulate apoB gene expression and to treat hyperlipidemia.

Our ultimate goal of using apoB mRNA-specific hammerhead ribozyme as a gene therapy agent is to investigate the long-term effect of decreasing apoB mRNA levels on the development of atherosclerosis. Our laboratory,[9–12] as well as others,[13] developed an atherosclerosis-prone LDb mouse model by deleting the LDL receptor (_Ldlr$^{-/-}$_) and apoB mRNA editing enzyme (_Apobec1$^{-/-}$_). In contrast to _C57BL/6_ wild-type or _Ldlr$^{-/-}$_ mice, the phenotype of the LDb mice (_Ldlr$^{-/-}$Apobec1$^{-/-}$_) closely mimics humans with hyperlipidemia characterized by the secretion of apoB100-containing lipoprotein only, with increased plasma levels of LDL cholesterol and decreased levels of high-density lipoprotein–cholesterol. In addition, these LDb mice spontaneously develop severe atherosclerotic lesions, even when feed on a normal chow diet. Thus, the LDb mouse would be a good model to study the effect of apoB mRNA-specific hammerhead ribozyme on atherosclerosis development.

In the current study, we have identified another ribozyme target site at 5′ region of apoB mRNA at GUC^{2326} (designated

[1]Center for Human Genetics, Brown Foundation Institute of Molecular Medicine, the University of Texas Health Science Center, Houston, Texas, USA; [2]Graduate School of Biomedical Sciences, the University of Texas Health Science Center, Houston, Texas, USA; [3]Division of Biostatistics and Human Genetics Center, School of Public Health, the University of Texas Health Science Center, Houston, Texas, USA; [4]Department of Biochemistry and Molecular Biology, and Center for Cardiovascular Research, Saint Louis University, St Louis, Missouri, USA; [5]Current Address: Qiqihar Medical University, Heilongjiang Province, P.R. China. Correspondence: Ba-Bie Teng, Center for Human Genetics, Suite 530D, Brown Foundation Institute of Molecular Medicine, the University of Texas Health Science Center at Houston, Houston, Texas 77030, USA. E-mail: babie.teng@uth.tmc.edu

as RB1), which cleaved apoB mRNA as efficiently as RB15. We delivered RB1, RB15, and the combination of RB1/RB15 using self-complementary adeno-associated virus 8.2 (scAAV8.2) vector to LDb mice to evaluate their effects on atherogenesis. We achieved our goal by demonstrating the therapeutic effect of apoB mRNA-specific hammerhead ribozymes of RB1, RB15 as well as the combination of RB1/RB15 in inhibiting the development of atherosclerosis. Interestingly, active ribozyme expression significantly decreased the triglyceride levels (TAG) in LDb mice. This is probably the result of decreased gene expression of diacylglycerol acyltransferase 1 (Dgat1) levels. This is the first time a study demonstrated a direct relationship between plasma triglyceride concentration and atherosclerosis, and the impact of decreasing apoB production on atherogenesis.

Results
Hammerhead ribozymes targeted at N-terminal (GUC^{2326}) and C-terminal (GUA^{6679}) of apoB mRNA efficiently decreased apoB mRNA expression in HepG2 cells
A schematic diagram showing the two ribozyme-targeted sites of ribozyme GUC^{2326} (designated as RB1) and ribozyme GUA^{6679} (designated as RB15) on apoB mRNA is depicted in **Figure 1**. The structure of RB15 was published previously by us.[8] The cleavage specificity of RB1 and RB15 is described in

the Materials and Methods section. **Figure 1a** shows a representative polyacrylamide gel analysis of *in vitro* ribozyme catalytic activity demonstrating that RB1 cleaved apoB RNA at GUC^{2326} efficiently to fragments of 235 and 176 nucleotides ($80 \pm 3.1\%$, $n = 5$) at 37 °C in 1 hour. As expected, the proportion of cleaved apoB RNA increased to $95 \pm 2.3\%$ ($n = 5$) at 50 °C. In comparison, RB15 cleaved $46 \pm 7.1\%$ ($n = 5$) of apoB RNA at 37 °C in 1 hour. The cleavage activity increased to $96 \pm 3.4\%$ ($n = 5$) at 50 °C. Thus, the *in vitro* cleavage activity demonstrated that both RB1 at GUC^{2326} and RB15 at GUA^{6679} cleaved apoB RNA substrate efficiently and ribozyme RB1 was more efficient at cleaving apoB RNA than that of RB15. Control experiments using antisense ribozyme RNA showed no detectable cleavage activity.

Next, we produced the recombinant adenoviruses expressing the corresponding ribozymes RB1, RB15, and RB15 mutant (Ad-RB1, Ad-RB15, and Ad-RB15 mutant, respectively). The RB15 mutant was constructed by substituting the G5 in the catalytic domain with an A (G5A), which abolished the cleavage activity as described previously.[8] HepG2 cells were infected with 2×10^9 particles of Ad-RB15 mutant as the inactive ribozyme, and Ad-RB1, Ad-RB15, and combination of Ad-RB1/Ad-RB15 as active ribozymes. At 24 hours after infection, total RNA was extracted from cells, and apoB mRNA levels were measured by using real-time
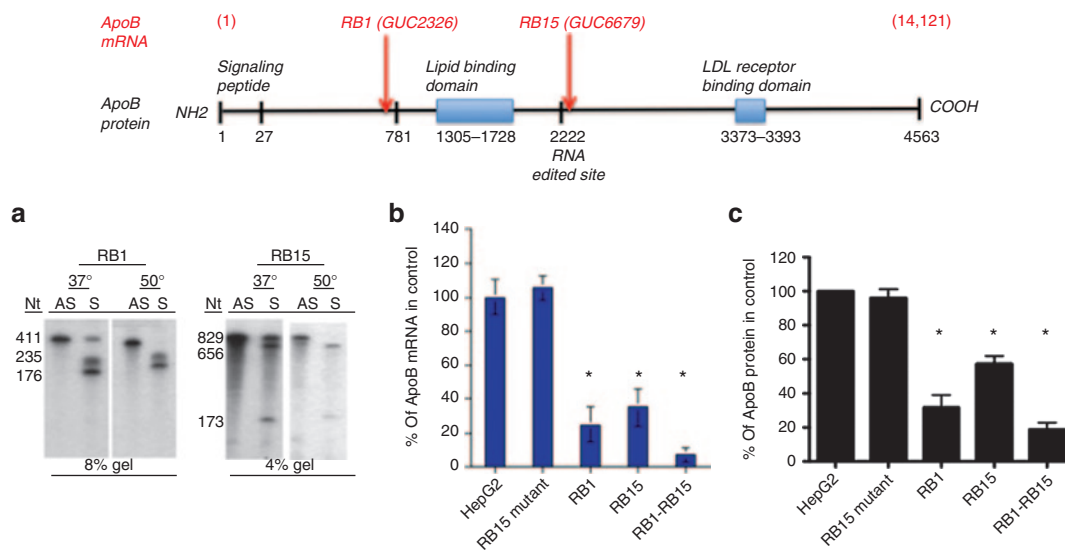

Figure 1 Effect of ribozymes on apoB mRNA levels. A schematic diagram of the location of apoB mRNA-specific ribozymes RB1 and RB15 is shown on the top. **a**) *In vitro* ribozyme cleavage assay. A substrate of apoB synthetic RNA of 411 nucleotides for RB1 and 829 nucleotides for RB15 was labeled with ^{32}P-UTP. *In vitro* ribozyme cleavage reaction was performed with 1×10^5 cpm of apoB RNA and 2 µg of corresponding sense (S) ribozyme RNA-RB1 or -RB15 in a 20-µl–reaction buffer. The reaction was carried at the indicated temperatures (37 or 50 °C) for 1 hour. Control experiments were carried out using antisense (AS) ribozyme RNA (2 µg). The reaction mixture was analyzed with 8% or 4% polyacrylamide urea gel electrophoresis and subjected to autoradiogram. Ribozyme RB1 RNA cleavage generated apoB fragments of 235 and 176 nucleotides, and ribozyme RB15 cleavage generated apoB fragments of 656 and 173 as described before.[8] The sizes of apoB RNA and cleaved RNA fragments are marked. The figures show a representative experiment. (**b**) Effect of ribozymes on apoB mRNA levels in HepG2 cells. HepG2 cells were plated onto 12-well culture plate. Cells were infected with 2×10^9 particles/well of Ad-RB1, Ad-RB15, combined Ad-RB1/RB15, or Ad-RB15 mutant for 15 hours. Control experiments are cells treated with phosphate-buffered saline only. The total RNA was extracted from each well, and apoB mRNA and endogenous 18S RNA from each well was determined by real-time quantitative PCR. The results are expressed as the percentage of apoB mRNA in Control (HepG2 cells treated with PBS). *The value of $P < 0.05$ is considered significant. The error bar represents SD. (**c**) Effect of ribozymes on apoB protein levels in HepG2 cells. The same experiments were performed as in **b** After the treatment, cell lysates were collected using RIPA buffer (Invitrogen), followed by ProSieve (6%) gel electrophoresis on cell lysates (50 µg/well) to separate apoB. The apoB protein was detected using anti-human apoB antibody and the intensity of the band was determined using LI-COR. The results are expressed as the percentage of apoB in control (HepG2 cells treated with PBS). *The value of $P < 0.05$ is considered significant. The error bar represents SD. apoB, apolipoprotein B; PBS, phosphate-buffered saline.

quantitative PCR. As shown in **Figure 1b**, the levels of apoB mRNA decreased markedly after active ribozymes treatment; apoB mRNA levels in RB1-treated cells decreased to $25\pm10\%$ of the nontreated control, that in RB15-treated cells was $35\pm11\%$, and that in the combined ribozymes RB1/RB15-treated cells was $7.4\pm4\%$. Cells treated with inactive ribozyme RB15 mutant increased slightly to $105\pm7\%$. Thus, both ribozymes RB1 and RB15 markedly reduced apoB mRNA levels, and importantly, the combined expression of ribozymes RB1/RB15 demonstrated a noticeable synergetic effect on reducing the apoB mRNA levels. The effects of ribozymes, RB1, RB15, and combination of RB1/RB15 on decreasing apoB mRNA levels were corroborated by the levels of apoB proteins (**Figure 1c**); the levels of apoB proteins were decreased significantly to $34\pm15\%$, $58\pm12\%$, and $20\pm5.8\%$ after ribozymes treatment of RB1, RB15, and combined RB1/RB15, respectively. Similar to the effect on apoB mRNA, the levels of apoB protein in RB15 mutant–treated cells increased slightly to $106\pm9.6\%$.

Long-term expression of apoB mRNA-specific ribozymes via scAAV8.2 vectors decreased apoB mRNA levels in mice

The goal of this study was to investigate the long-term effect of expressing apoB-specific hammerhead ribozymes on atherosclerotic lesion development. We then constructed RB1, RB15, and RB15 mutant using scAAV8.2 vectors to achieve efficient long-term gene expression in the liver in mice. We transduced scAAV8.2-RB1, scAAV8.2-RB15, the combination of scAAV8.2-RB1 and scAAV8.2-RB15 (comb), or scAAV8.2-RB15 mutant to LDb mice ($Ldlr^{-/-}Apobec1^{-/-}$)[9–12,14] at 2 months of age ($n = 11$/group). The study was ended at 4 months after transduction, because by 6 months of age, the untreated LDb mice would have developed severe atherosclerotic lesions. At 4 months after ribozymes transduction, the ribozymes levels were readily detectable in the liver of treated mice (RB1, RB15, RB1/RB15, and RB15 mutant) as demonstrated by RT-PCR followed by radioactive hybridization analysis with the corresponding ribozyme (**Figure 2a**). We also used real-time quantitative PCR to quantify the levels of ribozyme RNA expressed in the liver. As shown in **Figure 2b**, ribozyme RNAs were detected at both days 30 and 120 after treatment. The ribozyme RB1 was expressed at twofold higher than RB15 or RB15 mutant, which may suggest that RB1 is expressed more efficiently than RB15. As expected, the combined ribozymes RB1/RB15 had higher expression levels than a single ribozyme. These results indicated that in the liver of LDb mice, the scAAV8.2 cytomegalovirus (CMV) promoter vector expressed ribozymes efficiently at least for 4 months.
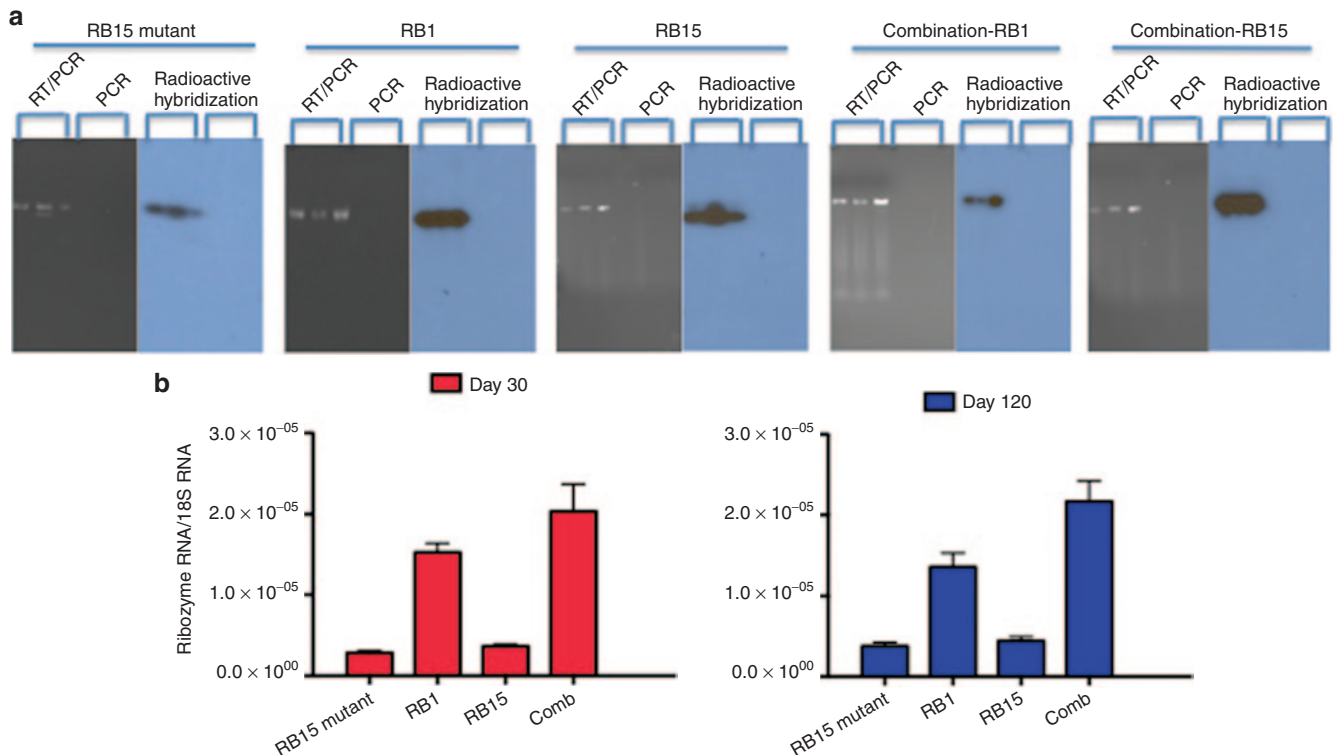

Figure 2 The expression of ribozyme RNAs in the liver of LDb mice after the corresponding scAAV8.2 ribozyme treatment. (**a**) Each mouse was transduced with scAAV8.2-ribozyme 2×10^{11} particles/animal. At days 30 and 120 after treatment, the animals were killed and the liver from each animal was collected. Total RNA was extracted from the liver of each mouse, and the expression of ribozyme RNA (RB15 mutant, RB1, RB15, and combination of RB1/RB15) was detected by RT-PCR, followed by ³²P-labeled corresponding ribozyme hybridization analysis. The radioactive bands of ribozymes RB15 mutant, RB1, RB15, and combination of RB1/RB15 are shown. The RNA samples were also subjected to PCR only, followed by radioactive hybridization analysis. There were no detectable bands in these samples. (**b**) The ribozyme RNA was determined using real-time quantitative PCR. The primers were designed against the poly-A sequences (**Table 1**). The ribozyme RNA levels are expressed as the ratio of ribozyme RNA normalized with 18S RNA. The results are expressed as mean ± SD. apoB, apolipoprotein B.

Table 1 The nucleotide sequences of primers and probes that used for real-time qPCR

Gene symbol	Primer and probe sequences	Optimized concentration (µmol/l)
mApoB (for RB15 cleavage site)	Forward: 5′GTC AAT GGC CGA GTT CCA GAT	2.50
	Reverse: 5′TCA CCA TGT CCT GTT CAT GCT T	2.50
	Probe: /5′6-FAM/TGG ACC ACT/ZEN/TTG GCT ATA CTA CAG ATG/3IABkFQ/	1.20
mApoB (for RB1 cleavage site)	Forward: 5′ATGTACTAATTGCCATAGATAGTGCCA	2.50
	Reverse: 5′TCGCGTATGTCTCAAGTTGAGAG	2.50
	Probe: 6FAM-ATCAACTTCAATGAAAAA MGBNFQ	1.20
Dgat1	Forward: 5′GGCATTCACAGCAATGATGGC	2.00
	Reverse: 5′CCACACAGCTGCATTGCCATA	2.00
16S	Forward: 5′AGGAGCGATTTGCTGGTGTGG	1.00
	Reverse: 5′GCTACCAGGGCCTTTGAGATG	1.00
18S	Forward: 5′TAACGAACGAGACTCTGGCAT	2.50
	Reverse: 5′CGGACATCTAAGGGCATCACA	2.50
	Probe: /5′6-FAM/TGG CTG AAC/ZEN/GCC ACT TGT CCC TCT AA/3IABkFQ/	1.25
HSVTKpA	Forward: 5′CCG TGC GTT TTA TTC TGT CTT TT	2.0
	Reverse: 5′GAA GGA GAC AAT ACC GGA AGG A	2.0

The optimized concentrations for each primer and probe are listed in the table. The primer and probes are synthesized by Integrated DNA Technologies (Coralville, IA).
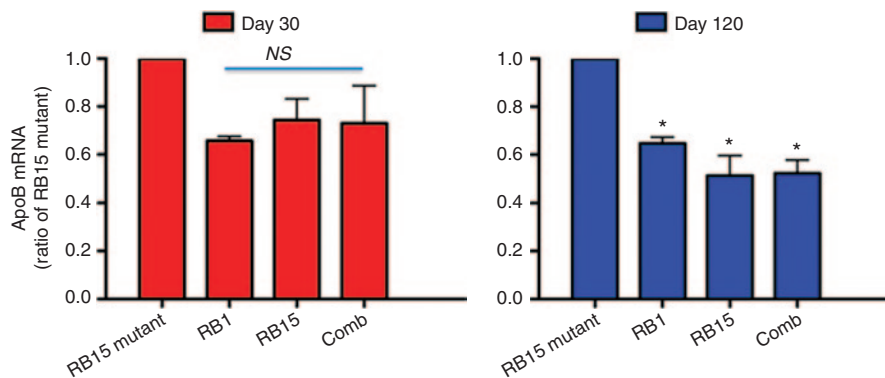ApoB, apolipoprotein B; Dgat1, diacylglycerol acyltransferase 1.

Figure 3 The expression levels of apoB mRNA after scAAV8.2 ribozyme treatment. LDb mice at 2 months of age were transduced with scAAV8.2-ribozyme 2×10^{11} particles/animal (RB15 mutant, RB1, RB15, or combination of RB1/RB15 groups). At the indicated time (days 30 and 120 after treatment), animals from each group were killed and liver total RNA was extracted from each animal. We used real-time quantitative PCR to determine the levels of apoB mRNA. The results were normalized with 18S RNA and expressed as the ratio of active ribozymes/control inactive ribozyme RB15 mutant. The differences were analyzed by two-sample *t*-test and the *P* values of <0.05 are considered significant (at days 120, the *P* values of RB1, RB15, and comb of RB1/RB15 versus RB15 mutant are 0.0377, 0.0148, and 0.0183, respectively). The error bar represents SD. apoB, apolipoprotein B; NS, not significant.

Next, we examined whether the active ribozymes inhibit the expression of apoB mRNA in LDb mice. As shown in **Figure 3**, at day 30 after active ribozymes treatment, the levels of apoB mRNA decreased in comparison with the groups treated with inactive ribozyme RB15 mutant, but the reduction did not reach statistically significant level of 0.05. It is probably due to a small number of animals ($n = 3$/group) killed at day 30. However, at day 120 after treatment, the apoB mRNA levels in mice treated with active ribozymes of RB1, RB15 or combined RB1/RB15 were significantly decreased to 35, 48, and 48%, respectively, compared with mice treated with control inactive ribozyme RB15 mutant ($P = 0.0016$). Thus, ribozymes RB1, RB15, or combined RB1/RB15 were catalytically active *in vivo*; they cleaved apoB mRNA and resulted in substantially decreased of apoB mRNA levels.

Effects of scAAV8.2-RB1, RB15, and combined RB1/RB15 on the concentrations of lipids and plasma apoB
We studied the effects of active ribozymes on body weight, plasma cholesterol, triglyceride, and apoB levels in LDb mice. There was a steady significant increase in body weights from day 0 before treatment to day 120 after treatment in all the groups studied ($P < 0.0001$), but there was no significant difference among the four groups studied (RB1, RB15, combined RB1/RB15, and RB15 mutant) (**Figure 4a**).

The plasma cholesterol levels changed significantly versus the time in control RB15 mutant, RB15, and combined RB1/RB15 groups, except RB1. In comparison with control inactive RB15 mutant group, both RB1 and combined RB1/RB15 treatment had significantly decreased cholesterol levels ($P = 0.0018$, 0.0378, respectively) but not the RB15 treatment group
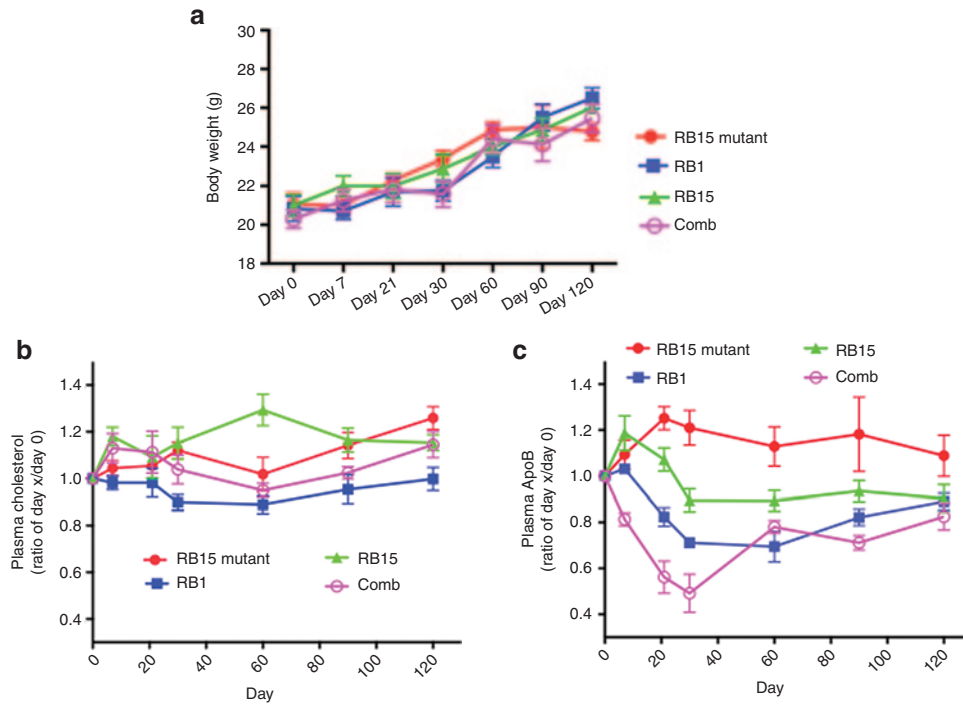
Figure 4 Analysis of body weight, plasma cholesterol, and apoB levels in LDb mice after scAAV8.2-ribozyme treatment. (a) The body weight (g) and the concentrations of plasma cholesterol and apoB were determined (mean ± SD) from each animal after treatment with RB15 mutant (closed circle), RB1 (closed square), RB15 (closed triangle), and combination of RB1/RB15 (open circle). **(b)** Plasma cholesterol and **(c)** apoB values are computed as the ratio of the day after treatment/day 0 before treatment. The statistic analyses of all the samples were performed using a linear mixed model including both fixed effects and random effects. Linear, quadratic, and cubic time curves were fitted and the best model was determined using F-tests. The P values of each group are described in the text. The error bar represents SD. apoB, apolipoprotein B.

(**Figure 4b**). Taken together, the result in RB1 group suggests that RB1 treatment is more efficient to resist the increase of cholesterol levels as the function of age.

Next, we determined the plasma apoB levels after ribozymes treatment (**Figure 4c**). The plasma apoB levels changed significantly versus time in all the active treatment groups of RB1, RB15, and combined RB1/RB15 ($P < 0.0001$), but not in control RB15 mutant group. When we compared the active ribozymes groups with inactive RB15 mutant group, the plasma apoB levels in LDb mice were significantly decreased after the treatment with active ribozymes of RB1 ($P < 0.0001$), RB15 ($P = 0.0076$), and combination of RB1/RB15 ($P < 0.0001$).

In comparison with day 0 before treatment, the plasma apoB levels decreased 30% by day 30 after RB1 treatment, and the levels remained at 20% by day 120. The plasma apoB levels in the RB15 ribozyme group decreased ~10% at day 30 compared with day 0 before treatment and remained at that level throughout the study. The combined ribozymes RB1/RB15 treatment group had the most marked decrease in apoB levels; at day 21 after treatment apoB levels reduced to 56% of that in day 0, and it remained at 30% of day 0 levels throughout the study. The decreased in plasma apoB levels is likely to be the consequence of active ribozymes cleaving apoB mRNA and decreasing the levels of apoB mRNA. Moreover, the active ribozyme RB1 was more efficient to reduce the apoB levels than that of RB15, and the comb group (RB1/RB15 treatment) had the best effect on reducing the apoB

levels. In contrast, LDb mice treated with inactive ribozyme RB15 mutant had increased levels of apoB, and the levels remained elevated through out the study. The increased levels of cholesterol and apoB in mice treated with inactive ribozyme RB15 mutant were also observed in our previous study using adenovirus as a vehicle.[7]

Most interestingly, the plasma TAG decreased significantly in all the groups treated with active ribozymes; RB1 ($P < 0.0001$), RB15 ($P = 0.0001$), and combination of RB1/RB15 ($P = 0.0003$), compared with day 0 before treatment (**Figure 5**). The TAG in RB1-treated group decreased 29% immediately at day 7 after treatment, and the levels continued to decrease to 40% and remained at that level by day 120. The TAG in RB15-treated group started to decrease to 30% by day 30 and remained relatively at that level by day 120. Similar to RB1 group, the TAG in the combined RB1/RB15 group decreased 20% at day 7 after treatment, and the levels further decreased to 30% and remained at that level by day 120. In contrast, the TAG in the inactive ribozyme RB15 mutant–treated group increased significantly by day 90 and day 120 ($P < 0.0001$). In comparison with RB15 mutant group, the plasma TAG in the active ribozymes treated group were significantly reduced (RB1, $P = 0.0399$; RB15, $P = 0.0288$, and combined RB1/RB15, $P = 0.0306$).

As shown in **Figure 6**, fraction of plasma lipoproteins by fast protein liquid chromatography showed that the TAG in very low density lipoproteins (VLDL) decreased after treatment at days 30, 60, and 120 in all the active ribozymes
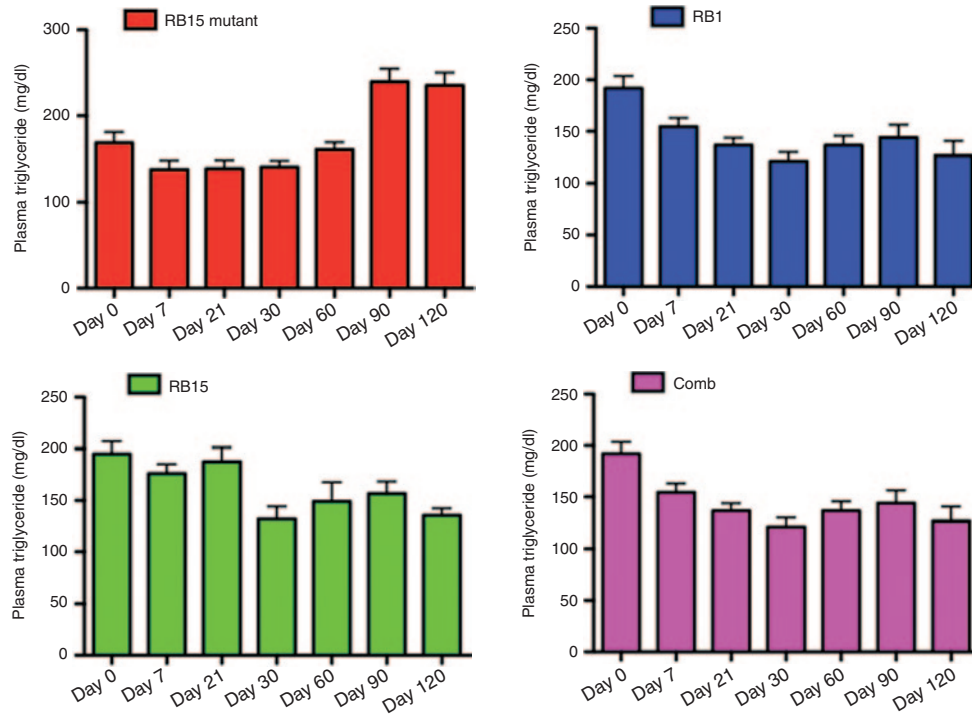
Figure 5 Analysis of plasma triglyceride levels in LDb mice after scAAV8.2-ribozyme treatment. The concentrations of plasma triglyceride (mg/dl) in LDb mice before the treatment (day 0) and indicated time after the treatment are shown in the figure. The results are shown as mean ± SD. The statistic analysis was performed as described in **Figure 4**, and the *P* value of each group is described in the text.
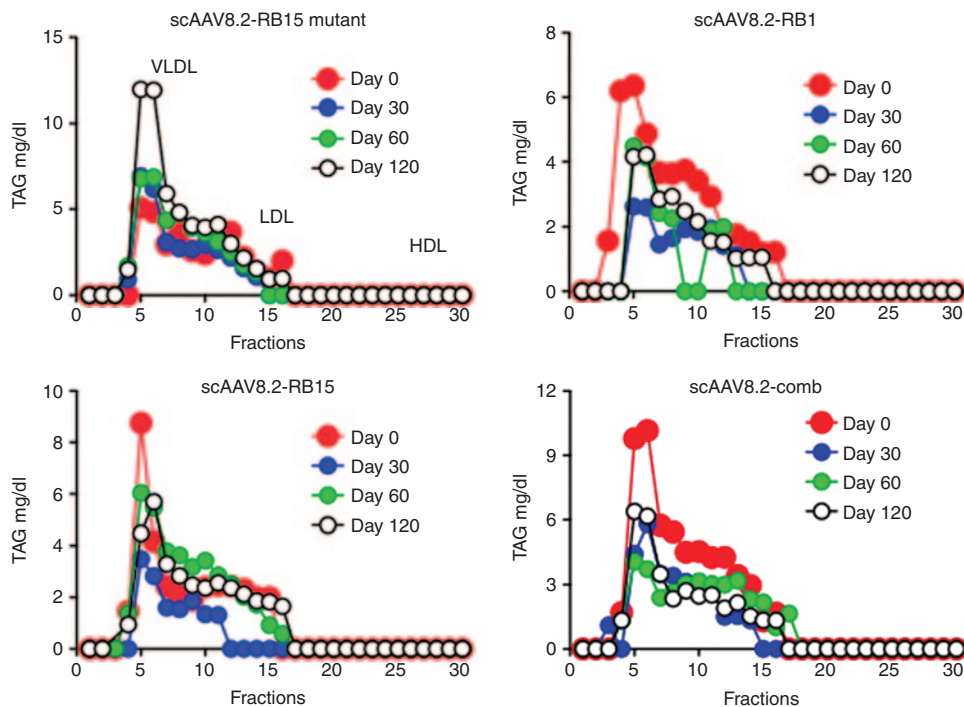

Figure 6 Distribution of triacylglycerol in plasma lipoproteins separated by FPLC. LDb mice were transduced with active ribozymes scAAV8.2-RB1, scAAV8.2-RB15, and comb scAAV8.2-RB1/RB15 or inactive ribozyme scAAV8.2-RB15 mutant. Pooled plasma samples (225 µl) from each group at indicated time were fractionated by FPLC. TAG levels from each fraction were measured and expressed as mg/dl. Positions of VLDL, LDL, and HDL are marked. FPLC, fast protein liquid chromatography; HDL, high-density lipoprotein; TAG, total triacyglycerol; VLDL, very low density lipoprotein.

groups, RB1, RB15, and comb RB1/RB15. In contrast, VLDL levels in the inactive RB15 mutant group did not change, but increased at day 120, which corresponded to the plasma TAG. Taken together, the long-term gene expression of active ribozymes RB1, RB15, and combined RB1/RB15 efficiently decreased apoB mRNA levels, resulting in reduced levels of plasma apoB and triglyceride.

Effect of scAAV8.2-RB1, RB15, and combined RB1/RB15 on atherogenesis

We then investigated whether the long-term gene expression of ribozymes targeted at apoB mRNA would result in decrease of atherosclerosis development in LDb mice. We quantified the atherosclerotic lesions in mice at day 120 after the treatment (6 months of age) with either control vector inactive ribozyme RB15 mutant, or active ribozymes including RB1, RB15 and combined RB1/RB15. As shown in **Figure 7a**, we quantified the total lesions in the whole aorta of LDb mice using en-face quantification method. At day 120, the atherosclerotic lesions covered >10% of the entire aorta ($10 \pm 0.8\%$) in LDb mice treated with control vector of inactive ribozyme RB15 mutant, whereas the LDb mice treated with active ribozymes RB1, RB15 or comb RB1/RB15 had very low amounts of lesions developed in
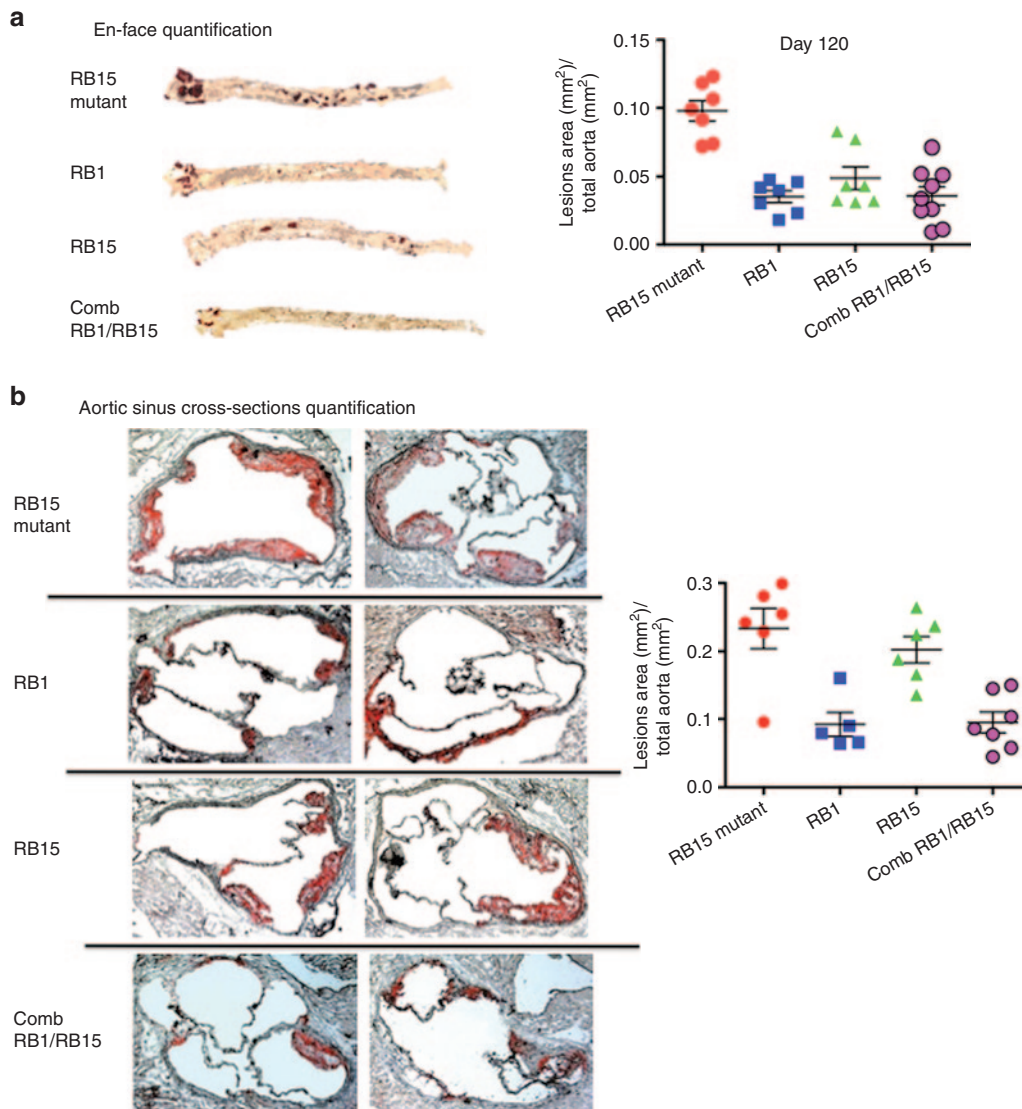

Figure 7 Quantification of aortic atherosclerotic lesion in LDb mice after scAAV8.2-ribozyme treatment. (**a**) En-face quantification of aortic atherosclerotic lesions. We quantified the lesions from the aortic arch to the iliac bifurcation. The results were presented as the aortic surface covered by lesions (mm^2) divided by the total surface area of the aorta (mm^2). A representative of the whole aortic tree stained with oil red O from each group (RB15 mutant, RB1, RB15, and combination of RB1/RB15) is shown. The right panel shows the ratio of lesion development from each animal at day 120 after treatment. The results of the statistical analysis are described in the text. The results of mean ± SD are shown. (**b**) Quantification of atherosclerotic lesions in the aortic sinus. The cross-sections of aortic sinus from each animal at day 120 after treatments were stained with oil red O. Representative of aortic sinus cross-sections stained with oil red O from two different animals of each group is shown in the left panel. The ratio of atherosclerotic lesions area/total cross-section area of each animal is shown in the right panel. The results of the statistical analysis are described in the text. The results of mean ± SD are shown.

the aorta (3.5±0.4%, 4.9±0.8%, 3.6±0.7%, respectively with $P < 0.0001$, 0.009, and <0.0001). A representative of aorta stained with oil red O from each group is shown in **Figure 7a** (left panel). Thus, our results demonstrated that active ribozymes treatment significantly decreased atherosclerotic lesion development.

We also quantified the lesions from the cross-sections of the aortic sinus from each animal studied and representatives of oil red O stained cross-sections are shown (**Figure 7b**). The percentage lesions on the aortic sinus in RB1 and combined RB1/RB15 ribozymes group were significantly lower (2.5-fold less) than that in control vector RB15 mutant group (9.4±1.8%, 9.5±1.5% versus 23±3.0%; $P = 0.0037$ and 0.0011, respectively). Unlike the total lesion in the whole aortic tree, the lesions in aortic sinus of RB15 ribozyme–treated group (20±2.0%) were not significantly different than that of control vector RB15 mutant–treated group. Taken together, our results demonstrated that active ribozyme RB1 and combined RB1/RB15 ribozymes efficiently inhibited atherosclerosis development in LDb mice, whereas ribozyme RB15 was less efficient.

The mechanism that affects the development of atherogenesis
Our results demonstrated that active ribozymes RB1, RB15, and combined RB1/RB15 decreased apoB mRNA levels and apoB production in LDb mice. Also, the treatment revealed significantly decreased of plasma triglyceride but not plasma cholesterol levels, which suggested that the reduction in apoB production decreased triglyceride biosynthesis. Dgat catalyzes the formation of triglycerides from diacylglycerol (DAG) and acyl-CoA. This is the committed step in triglyceride synthesis. We quantified the Dgat1 mRNA levels in the liver. As shown in **Figure 8**, as early as 30 days after treatment, the Dgat1 mRNA levels were significantly decreased in mice treated with active ribozymes RB1 ($P = 0.0226$), RB15 ($P = 0.0318$), and combined RB1/RB15 ($P = 0.0271$), when compared with the animals treated with control inactive ribozyme

RB15 mutant. The lower mRNA levels of Dgat1 persisted till day 120 after treatment.

Decreased Dgat1 has been shown to be atheroprotective;[15] we investigated whether ribozyme treatment had any effect on the levels of DAG molecular species. We examined DAG molecular species using electrospray ionization-tandem mass spectrometry as we have previously described.[16] As shown in **Figure 9**, the active ribozymes RB1, RB15, or combined RB1/RB15 markedly decreased murine liver DAG molecular species, compared with that in mice treated with inactive ribozyme RB15 mutant. The decreased DAG molecular species contained esterified fatty acids that included essential fatty acids such as linoleic acid (18:2, n-6), arachidonic acid (20:4, n-6), docosapentaenoic acid (22:5, n-3), and decosahexaenoic acid (22:6, n-3). The saturated fatty acids such as palmitic acid (16:0), stearic acid (18:0), and unsaturated fatty acids such as palmitoleic acid (16:1, n-7), oleic acid (18:1), linoleic acid (18:2) were all decreased after the active ribozymes treatment. Strikingly, RB15 group had substantial lower amounts of the fatty acids on DAG including the atheroprotection ω-3 fatty acids such as 22:5 and 22:6,[17] and this might contribute to the higher levels of lesions in aortic sinus in RB15-treated group.

Others have shown that the deficiency of Dgat1 mRNA levels was associated with reduced lipid-induced inflammation and macrophages migration.[15,18] We stained the atherosclerotic lesions of ribozymes-treated groups with CD68 to examine the extent of macrophages migration and apoB for the uptake of LDL. As shown in **Figure 10**, we detected a substantial amount of macrophages (red stain) and apoB (green stain) in the atherosclerotic lesions of LDb mice treated with inactive ribozyme RB15 mutant, whereas, LDb mice treated with active ribozymes of RB1, RB15, or combination of RB1/RB15 had much less amount of macrophages and apoB detected in the lesions. Taken together, our results provided direct cause and effect relationship that decreasing apoB and TAG resulted in reduction of atherosclerotic lesions development.
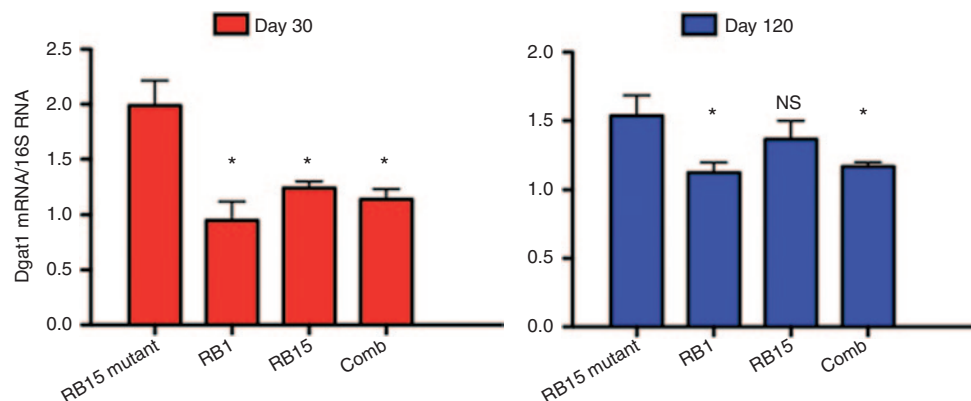

Figure 8 The gene expression levels of Dgat1 mRNA after scAAV8.2-ribozyme treatment. We used real-time quantitative PCR to determine the hepatic levels of Dgat1 mRNA in LDb mice after treatment with scAAV2/8-RB15 mutant, RB1, RB15, or combination of RB1/RB15 (comb) at days 30 and 120. The results are expressed as the ratio of Dgat1 mRNA/16S RNA. The statistical differences between RB15 mutant group versus RB1, RB15, and combination of RB1/RB15 were calculated using the t-test. *The P value of <0.05 is considered significant. The not significant value is listed as NS. The P values at day 30 of groups RB1, RB15, or comb versus RB15 mutant are 0.0226, 0.0318, and 0.0271, respectively. The P values at day 120 of groups RB1, RB15, or comb versus RB15 mutant are 0.0300, 0.4135, and 0.0171, respectively. The results of mean ± SD are shown. NS, not significant.
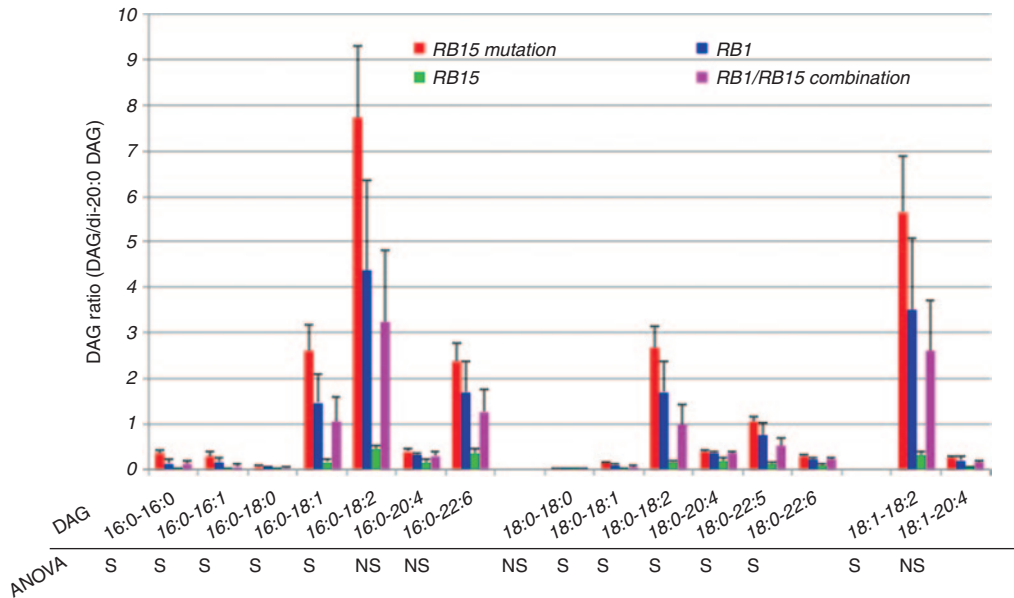
Figure 9 Alterations in liver diacylglycerol molecular species in LDb mice after scAAV8.2-ribozyme treatment. Total lipids were extracted from the liver of LDb mice at day 120 after treatment with either scAAV2/8-RB15 mutant, RB1, RB15, or combination of RB1/RB15 and subjected to shotgun lipidomics using a triple quadrupole electrospray ionization mass spectrometer with SRM of individual lithiated adducts of DAG molecular species as described in "Materials and Methods". The indicated DAG ratio is the ratio of the intensity of the SRM for the indicated DAG molecular species compared with that of the SRM intensity of the internal standard (di-20:0 DAG). Statistical differences between each treatment were determined using analysis of variance (ANOVA). The $P < 0.05$ are considered significant (S). The not significant value is listed as NS. The results of mean ± SD are shown. DAG, diacylglycerol; SRM, selected reaction monitoring.

Figure 10 The expression of CD68 and apoB in the atherosclerotic lesions in LDb mice after scAAV8.2-ribozyme treatment. We performed immunofluorescence staining of the aortic sinus cross-sections of LDb mice after treatment with scAAV8.2-RB15 mutant (control), or active ribozymes of RB1, RB15, or combination of RB1/RB15. The aortic sinus cross-sections were stained with CD68 (upper panel) and apoB (lower panel). The images were captured using a Zeiss Axio observer (Zeiss). D1m fluorescence microscopy with DAPI, FITC, and Texas Red filters. Final original magnification was ×5. apoB, apolipoprotein B.

Discussion

This study utilized the scAAV8.2 vector to express ribozymes targeted at apoB mRNA in atherosclerosis-prone LDb mice ($Ldlr^{-/-}Apobec1^{-/-}$), leading to a reduction in the concentration of plasma triglyceride and apoB, but not plasma cholesterol. Importantly, this is the first long-term study demonstrating that decreased apoB mRNA production, results in decreased atheroscleroticlesion development in atherosclerosis-prone LDb mice. We established that the consequence of reducing

apoB mRNA leads to decreased Dgat1 mRNA, reduction in inflammatory markers and atherosclerotic lesions development. Most intriguingly, the amounts of most of the free fatty acids on DAG were decreased significantly after the ribozyme treatment, which suggests that apoB regulates both energy storage and inflammatory response to the arterial wall. Taken together, the regulation of apoB mRNA levels has a direct effect on the development of atherosclerosis.

Atherosclerosis is characterized by a constant insult of inflammation on the arteries, and it has been established that

this inflammation primarily is caused by an accumulation/retention of LDL in the artery wall.[19,20] ApoB is the structural protein of LDL and elevated levels of apoB or LDL are positively associated with cardiovascular disease.[21–23] Today, lipid-lowering drugs such as statins are the most effective pharmaceutical treatment for regulating LDL cholesterol levels. However, a better strategy to regulate LDL levels would be to inhibit apoB production. Accordingly, Mipomersen, an antisense oligonucleotide was developed to target at apoB mRNA and lower LDL cholesterol levels in patients with familial hypercholesterolemia.[24,25] Many groups used siRNA to silence apoB mRNA to lower plasma cholesterol in mice.[26–29] Our laboratory has previously designed hammerhead ribozyme targeted at apoB mRNA at GUA[6679] (RB15) to demonstrate that ribozyme cleaves apoB mRNA at the specific site and decreases cholesterol, triglyceride, and apoB levels in a human apoB transgenic mouse model.[7,8] Our ultimate goal is to investigate whether inhibiting apoB mRNA expression would produce therapeutic effect on reduction in atherosclerosis development. We have used scAAV2 vector to express apoB mRNA-specific hammerhead ribozyme, but the low expression of AAV2 vector did not yield the therapeutic effect on atherosclerosis development.[14] In the current study, we used scAAV8.2 vector, which has been shown to efficiently transduce hepatocytes,[30–32] to express apoB mRNA-specific hammerhead ribozymes and demonstrated their therapeutic effects on decreasing the development of atherosclerosis. Thus, this study also provided the evidence that selection of the proper vector for gene delivery is the most important initial step for therapeutic treatment.

The unexpected discovery in this study was to find out that cleavage of apoB mRNA resulted in reduction of apoB production and markedly decreased of TAG (>30%) in LDb mice. The decrease in TAG was the consequence of decreased Dgat1 mRNA expression. There are two enzymes Dgat1 and Dgat2, which catalyze the esterification of diacyglycerol to triglyceride. Dgat1 is suggested to be involved in the recycling of free fatty acids from triglyceride to re-esterifying the monoacylglycerol and DAG.[33] A recent study shows that apoE^{−/−} mice deficient of Dgat1 (*ApoE^{−/−}Dgat1^{−/−}*) have reduced atherosclerosis.[15] This is the result of decreased inflammatory factors including decreased macrophages, and reduced expression of VCAM1, P-selectin, E-selectin, and MCP1 in the aorta. In our study, we showed a decreased deposit of macrophages and apoB in the atherosclerotic lesions in mice treated with active ribozymes. Dgat1 is currently a target of small molecule inhibitors for the treatment of diverse metabolic disorders.[34,35] As noted in this study, it is possible that the decreased Dgat1 expression may be the result of a negative feedback from the increased intracellular TAG levels in the liver, resulting from the inhibition of VLDL assembly by ribozyme activity.

Sequence-specific cleavage is a fundamental nucleic acid reaction. The hammerhead ribozyme has been the first catalytic structure whose structure was determined. The minimal hammerhead has been used to design target-specific ribozyme for therapeutic purpose. These small RNA units can achieve high sequence specificity and catalytic efficiency. Furthermore, these molecules are easy to design. The only drawback in ribozyme is to identify the RNA sequences that are open for binding *in vivo*. In this study, we show that ribozyme RB1 (*GUC2326*) is more efficient than RB15

(*GUA6679*) in treatment. There are potential three reasons for the differences. First, it is known that GUC cleaves target mRNA more efficiently than other sequences including GUA. Second, the RB1 cleavage site is located in the 5′ region beyond the lipid-binding domain of apoB mRNA (**Figure 1**), resulting in decreased assembly and secretion of VLDL and decreased plasma TAG. Finally, ribozyme RB1 is more efficiently expressed than RB15. Thus, this study further provides the importance on designing the best therapeutic target for effective treatment.

The difficulty in designing ribozyme can be resolved by the usage of ribozyme libraries in cell culture factors, which would accelerate the selection for the target sites on the RNA.[6] Recently, a new selection strategy, termed compartmental bead-tagging technology, in combination with RNA engineering, can yield polymerase ribozymes that display enhanced polymerase activity and fidelity, as well as generality, and allow the ribozyme-catalyzed transcription of an active ribozyme from an RNA template.[36] This would transform the ribozyme inhibition technology in the future to address therapeutic approach to human diseases.

Materials and methods

Cell lines and culture. Human hepatocellular carcinoma cell line (HepG2; American Type Culture Collection, Manassas, VA) was cultured in Eagle's minimum essential medium containing 10% fetal bovine serum, 2 mg/ml glutamine, 50 units/ml penicillin, 50 mg/ml streptomycin, 1 mmol/l sodium pyruvate, and 0.1 mmol/l nonessential amino acids. Cells were cultured at 37 °C with 5% CO_2 environment.

Molecular engineering and virus production
Plasmid construction of ApoB mRNA-specific hammerhead ribozymes: Dr Teng's laboratory has previously published the apoB mRNA-specific hammerhead ribozymes targeted at GUA 6679 of the apoB mRNA, designated RB15.[8] A point mutant of the conserved catalytic domain at nucleotide G[5] to A (G5A) of the RB15 is designated as RB15 mutant.[8] In this study, we generated another apoB hammerhead ribozyme targeted at sequences of GUC2326, designated as RB1. The numbering of apoB corresponds to the published human apoB100 sequence[37] (GenBank accession number X04506). These three constructs were cloned into XbaI and ClaI sites of pGem 7Zf(+) vector (Promega, Madison, WI) to synthesize synthetic ribozyme RNA. We have searched the gene bank using the sequences of RB15 and RB1, which had no matches. In our previous publication,[8] we used a reverse ligation-mediated PCR and confirmed by sequencing that RB15 ribozyme cleaves apoB mRNA at the exact target site of GUA 6679. In here, we performed a rapid amplification of 5′cDNA ends method (5′race), followed by sequencing to confirm the cleavage site of ribozyme RB1 on apoB mRNA. Briefly, we used the protocol described in *Molecular Cloning*.[38] We designed the following primers for this assay: apoB-gene–specific primer-1 (5′ GGA GCA ATG ACT CCA GAT GA), apoB-gene–specific primer-2 (5′ CAG GAG CTG GAG GTC ATG GA), apoB-sequencing primer (5′ AGATGCGGAGGTAGGCTCTG), and dT-17 adaptor primer (5′ GAC TCG AGT CGA CAT CGA TTT TTT TTT TTT TTT TT). We used GSP-1 to reverse

transcript total RNA from RB1-treated HepG2 cells to synthe-size the 1st cDNA. The cDNA was purified by using Qiagen PCR purification kit (Qiagen, Valencia, CA), and the prod-uct was added a homopolymeric dA tail to the 3′end using the terminal transferase (Fisher Scientific, Pittsburgh, PA). This product was, then, amplified in the presence of dt-17 adaptor primer and GSP-2 primer (94 °C 5 minutes; 94 °C 30 seconds, 58 °C 30 seconds, and 72 °C 45 seconds for 30 cycles, followed by 72 °C 5 minutes), which yield a PCR product of 186-bases long. We purified the PCR product by using Qiagen PCR purification kit (Qiagen), and the product was sequenced using apoB-sequencing primer by Lone Star Labs (Houston, TX). We confirmed ribozyme RB1 specifically cleaved apoB mRNA at the expected target site GUC2326.

Construction of recombinant adenoviral ribozymes and Infection. ApoB hammerhead ribozymes, RB1, RB15, and RB15 mutant, were cloned into the adenoviral shuttle vector, pAvS6, which contains a Rous sarcoma virus promoter as described by Teng *et al.*[8,39] Briefly, the high titer recombinant adenovirus was produced and amplified on 293 cells and purified by CsCl gradient centrifugation as described previ-ously by Teng *et al.*[39]

HepG2 cells were plated onto six-well culture dishes until the cells reached 80% confluency. The cells were infected with 1×10^9 viral genome/ml of Ad-RB1, Ad-RB15, combined Ad-RB1–Ad-RB15, or Ad-RB15 mutant as indicated in each experiment. The HepG2 apoB mRNA levels were deter-mined by real-time quantitative RT-PCR using ABI7900 Sequence Detection System (Applied Biosystems, Fos-ter City, CA). The sequences-specific primers and probes used for human apoB mRNA and the endogenous control 18S ribosomal RNA were listed in **Table 1**. The results are expressed as the percentage of ribozyme-treated to non-treated HepG2 cells.

The cell lysates were also collected after adenovirus treat-ment and subjected to 6% ProSieve-50 gel electrophoresis (FMC Bioproducts, Rockland, ME) for apoB. The respec-tive proteins were detected by anti-human apoB antibody (Abcam, Cambridge, MA). The intensity of protein bands was semi-quantified using an Odyssey Infrared Imaging system (LI-COR, Linclon, NE).

scAAV8.2 viral vector production. The plasmid construction and viral vector production was performed by Virovek (Hay-ward, CA).

Construction of plasmid: Two oligos corresponding to RB1 were synthesized (first forward primer: 5′GGCCTCTAGAGT GGTCCACTAACTGATGAGTCCGTGA GGACGAAACCTT3′; second forward primer: 5′TCCGTGAGGACGAAA CCTTAG AGACAATCGATCATGGGGGAGGCTAACTGAAAC3′). They were used together with a reverse primer (5′ATATGCATGC-GCTTGCCGCCCCGA CGTTG3′) to amplify the HSVTK poly-A sequence. The resulting PCR fragment was cut with XbaI and SphI and ligated to the XbaI and SphI sites of pFB-sceGFP to create pFBscCMV-RB1. Similarly, two oligos corresponding to RB15 (first forward primer: 5′GGCCTCT AGAACTATCTTTAATACTGATGAGTCCGTGAGGACG AAACTGA3′; second forward primer: 5′GTCCGTGAGGAC GAAACTGATC AAATTGATCGATATGGGGGAGGCTAACTG AAA3′) and two oligos corresponding to RB15mutant

(fist forward primer: 5′GGCCTCTAGAACTATCTT TAATACT AATGAGTCCGTGAGGACGAAACTGA3′; second forward primer: 5′GTCCGTGAGGACGAAACTGATCAAATTGATCG ATATGGGGGAGGCTAAC TGAAA3′) were also synthesized and used in the same way to generate pFBscCMV-RB15 and pFBscCMV-RB15mutant. The regions corresponding to the oligo areas were DNA sequenced to verify the identity of the sequences.

Generation of recombinant baculoviruses and AAV8.2 vector production: The Virovek used the Bac-to-bac sys-tem as described by Invitrogen (Carlsbad, CA) to generate recombinant baculoviruses. The recombinant baculoviruses were amplified once and used for AAV production. Sf9 cells (Invitrogen) were cultured to 1×10^7 cells/ml and diluted to 5×10^6 cells/ml to be double infected with Bac-inRepOpt-hr2-inCap8.2 and Bac-sc-CMV-RB1, -RB15, or -RB15 mutant for 3 days to produce AAV 8.2 vectors. At 3 days after infection, the Sf9 cells were harvested and lysed in SF9 lysis buffer (50 mmol/l Tris–HCl, pH7.8, 50 mmol/l NaCl, 2 mmol/l $MgCl_2$, 1% DOC, 0.5% CHAPS, and 140 units/ml Benzonase) at 37 °C for 1 hour. Cell debris was removed by centrifugation at 8,000 rpm for 30 minutes. The cleared lysates were loaded onto CsCl step-gradient and centrifuged at 28,000 rpm for 20 hours. The viral band was loaded onto a second CsCl and centrifuged at 65,000 rpm for 24 hours. The viral band was passed through two PD-10 desalting columns (GE HealthCare, Munich, Ger-many) to remove the CsCl and detergents to exchange to phosphate-buffered saline buffer. The titer of the AAV vec-tor was quantified with the primers corresponding to CMV promoter (forward primer: 5′TAACGCCAATAGGGACTTTC CAT3′; reverse primer: 5′CGGTAGCCAAGTGGGCAGTT TACCG3′). SYBR green 2x Master mix was used for the qPCR assays. The titer was in the range of $0.5–1.0 \times 10^{13}$ viral genome/ml.

In vitro *ribozyme cleavage reaction.* The detail description of this assay was described previously by Tengs' laboratory.[8] Briefly, we used a maxiscript kit from Ambion (Austin, TX) to synthesize ribozyme RNA from the ribozyme plasmid vectors pRB1, pRB15, and pRB15 mutant using T7 RNA polymerase. The concentration of synthetic ribozyme RNA was determined by measuring optical density at 260 nm. Plasmid vector con-taining human apoB cDNA fragment was used to transcribe a ^{32}P-radiolabeled synthetic apoB RNA as the substrate. The *in vitro* assay was performed using 1×10^5 cpm ^{32}P-labeled apoB RNA as substrate and 2 µg of ribozyme RNA in a buf-fer containing 50 mmol/l Tris, pH7.5, 20 mmol/l $MgCl_2$, and 1 mmol/l EDTA. The reaction was carried out for 1 hour at either 37 or 50 °C as indicated. The products were analyzed using polyacrylamide urea gel electrophoresis. The gel was autoradiographed and quantified using PhosphoImager SI scanner (Molecular Dynamics, GE Healthcare Biosciences, Pittsburgh, PA).

Animal experiments. Mice deficient in both LDL recep-tor (*Ldlr*$^{-/-}$) and apoB mRNA editing enzyme (*Apobec1*$^{-/-}$) were generated in Teng's laboratory[9–11,14] and were used for this study. Mice were kept in a barrier facility with a 12:12-hour dark–light cycle, and maintained on a standard labo-ratory chow diet. All animal experiments were conducted

in accordance with the Guidelines of the Animal Protocol Review Committee of the University of Texas Health Science Center at Houston.

There were four groups of LDb mice for this study: scAAV8.2-RB1, scAAV8.2-RB15, combination of scAAV8.2-RB1 and scAAV8.2-RB15, and scAAV8.2-RB15 mutant as the control. LDb male mice (n = 11 per group) aged 2 months were transduced with AAV8.2 viruses as described (2×10^{11} viral particles per mouse) via tail vein injection. The animal received combination of scAAV8.2-RB1 and scAAV8.2-RB15 had 2×10^{11} viral particles of each ribozyme per mouse. Fasting (=16 hours) blood samples were collected pre- (day 0) and postviral injection on days 7, 21, 30, 60, 90, and 120 via retro-orbital plexus by using a heparin-coated capillary tube (Fisher Scientific). On day 30, three animals from each group were killed, and the liver and other organs were collected, snap-frozen in liquid nitrogen and stored at –80 °C. On day 120, all the rest of the animals were killed and samples were collected for the study. We used a quantitative real-time PCR method to determine the distribution of ribozyme vector in mice after treatment. As expected, substantial amounts of scAAV8.2 vector (~99%) were detected in the liver ($1–6 \times 10^4$ copy number/μg genomic DNA) and small amount was detected in the spleen ($0.8–2.5 \times 10^3$ copy/μg genomic DNA), small intestine ($1–5 \times 10^2$ copy/μg genomic DNA), kidney ($1–3 \times 10^2$ copy/μg genomic DNA), testis ($1–3 \times 10^2$ copy/μg genomic DNA), and heart ($1–4 \times 10^2$ copy/μg genomic DNA).

Analysis of plasma lipid and apoB levels. Plasma cholesterol and triglyceride concentration were determined using the Cholesterol E and the L-type Triglyceride M kits (Wako Chemicals, Richmond, VA), respectively.

Mouse plasma apoB (1 μl) was resolved by gel electrophoresis by using ProSieve-50 gel (6%) (FMC BioProducts). The apoB protein was detected by anti-mouse apoB (Abcam). The intensity of protein bands was semi-quantified using an Odyssey Infrared Imaging system (Li-COR).

Pooled plasma (225 μl) was separated by fast protein liquid chromatography on two Superose 6 columns (Amersham Biosciences, Piscataway, NJ). Fractions (0.5 ml each) were eluted using 150 mmol/l NaCl, 1 mmol/l EDTA, and 0.02% NaN$_3$ pH 8.2 to separate VLDL, LDL, and high-density lipoprotein.[7,11] The triglyceride concentration in each fraction was determined using L-type triglyceride M kits (Wako Chemicals).

Real-time quantitative PCR. Total RNA was extracted from mouse livers using Qiazol reagent (Qiagen), digested with DNase I (Ambion), and transcribed into cDNA using Achieve Reverse Transcription kit (Applied Biosystems). Real-time quantitative PCR (qPCR) was performed on ABI Prism 7900 Sequence Detection System (Applied Biosystems). RNA was quantified using the SYBR Green PCR Master Mix (Bio-Rad, Hercules, CA). Each primer set was optimized to eliminate primer-dimer formation. The mouse apoB mRNA levels were quantified using TagMan primers/probe. The results are expressed as the ratio of specific RNA/house keeping RNA. The mouse apoB RNA was normalized with 18S RNA. The Dgat1 mRNA was normalized with 16S RNA. The ribozyme RNA was determined using sequences obtained from HSVTK

poly-A and normalized with 18S RNA. Sequences of primers and probes used in this study are listed in **Table 1**.

Quantification of atherosclerotic lesions. We used two methods (en-face and aortic root cross-section) to quantify the atherosclerotic lesions. The en-face method is to quantify the atherosclerosis throughout the whole aortic tree (from the aortic valve to the bifurcation of the iliac arteries). The aortic root cross-section is to quantify the atherosclerotic lesions at the vessel origin. Both methods have been described in detail previously by Teng's laboratory.[14] The results are presented as the ratio of lesions (mm^2) divided by the total surface area of the aorta (mm^2). Two operators not knowing the sample origin performed the quantification of atherosclerotic lesions.

Immunofluorescence analysis on aortic sinus. Cryosections (5 μm) of aortic sinus were processed from each mouse. The sections were fixed in 4% buffered formalin phosphate for 10 minutes at room temperature. After washing, the sections were incubated with 1% bovine serum albumin phosphate-buffered saline–Tween 20 for 1 hour at room temperature to block nonspecific binding. The sections were then incubated at 4 °C overnight with the primary antibodies, 1:50 dilution of goat anti-mouse CD68 (Adb Serotec, Raleigh, NC), 1:100 dilution of rabbit anti-mouse apoB (Abcam). After washing, the slides were incubated with 1:150 Alexa-594 or Alexa-488 conjugated corresponding secondary antibodies (Invitrogen) for 1 hour at room temperature. The slides were subsequently washed and mounted with mounting media containing DAPI (Vector, Burlingame, CA) and examined using a Zeiss Axio observer (Zeiss, Thornwood, NY). D1m fluorescence microscopy with DAPI, FITC, and Texas Red filters. Control slides without primary or secondary antibodies were performed at the same time.

DAG analysis by mass spectrometry. Mouse liver was homogenized with phosphate-buffered LiCl (150 mmol/l, phosphate-buffered LiCl) at 4 °C (100 mg tissue/ml phosphate-buffered LiCl), and 100 μl were immediately subjected to a modified Bligh-Dyer extraction (1 mg/ml LiCl added to the water phase) in the presence of di-20:0 DAG internal standard.[40] Following collection of the organic phase, the upper phase was re-extracted with chloroform and the resultant organic phase was pooled with the initially collected organic extract. Pooled organic extracts (5 ml) were back extracted with 4 ml of 1 mg/ml LiCl. The chloroform phase was then sequentially collected, dried under nitrogen, suspended in 250 μl of chloroform, and stored under N$_2$ at –20 °C until analysis. Sixty microliters of the lipid extract was combined with 240 μl of methanol and 8 μl of 10 mmol/l LiOH in methanol before direct infusion electrospray ionization mass spectrometry (ESI-MS) using a Thermo Fisher Quantum triple quadrupole instrument. DAG molecular species were detected by selected reaction monitoring of their lithiated adduct parent ions coupled with their product ion representing the loss of one of the lithiated fatty acid residues as described previously.[16] For DAG molecular species containing mixed fatty acids including unsaturated fatty acids the product ion always represented the loss of the lithiated unsaturated fatty acid (as this provided the most stable product ion). DAG molecular species were quantified as a ratio of the intensity of their respective

selected reaction monitoring compared with that of the internal standard, di-20:0 DAG.

Statistical analysis. All results are expressed as the mean ± SD values. The change of body weight, plasma cholesterol, plasma triglyceride, or plasma apoB levels with time stratified by treatment were analyzed using a linear mixed model including both fixed effects and random effects. Linear, quadratic, and cubic time curves were fitted and the best model was determined using *F*-tests. Treatment effects of body weight, plasma cholesterol, plasma triglyceride, or plasma apoB levels were also analyzed using linear mixed model adjusting for time effects. Mixed model takes into account of correlations among repeated measurements taken from the same subject. It can also provide effect estimates of covariates, showing advantage over analysis of variance. All the analyses using mixed models were conducted using PROC MIXED procedure of SAS V9.2 (SAS Institute, Cary, NC). The significance of time effects or treatment effects was tested using *F*-tests and *P* value smaller than 0.05 was considered to be statistically significant.

Analysis of variance was used to compare ApoB and Dgat1 mRNA levels among different treatment groups on day 30 and on day 120 separately. *P* value <0.05 was considered to be statistically significant.

The comparison of atherosclerotic lesions of mice treated with control vector AAV2/8-RB15 mutant versus experimental groups of AAV2/8-RB1, AAV2/8-RB15, and combination of AAV2/8-RB1 and RB15 were performed using GraphPad Prism software (version 5; GraphPad Software, San Diego, CA) unpaired *t*-tests with two-tailed *P* values. *P* < 0.05 was considered to be statistically significant.

1. Ferré-D'Amaré, AR and Scott, WG (2010). Small self-cleaving ribozymes. *Cold Spring Harb Perspect Biol* **2**: a003574.
2. Uhlenbeck, OC (1987). A small catalytic oligoribonucleotide. *Nature* **328**: 596–600.
3. Haseloff, J and Gerlach, WL (1988). Simple RNA enzymes with new and highly specific endoribonuclease activities. *Nature* **334**: 585–591.
4. Mulhbacher, J, St-Pierre, P and Lafontaine, DA (2010). Therapeutic applications of ribozymes and riboswitches. *Curr Opin Pharmacol* **10**: 551–556.
5. Tschuch, C, Schulz, A, Pscherer, A, Werft, W, Benner, A, Hotz-Wagenblatt, A *et al.* (2008). Off-target effects of siRNA specific for GFP. *BMC Mol Biol* **9**: 60.
6. Unwalla, HJ and Rossi, JJ (2012). Screening effective target sites on mRNA: a ribozyme library approach. *Methods Mol Biol* **848**: 329–336.
7. Enjoji, M, Wang, F, Nakamuta, M, Chan, L and Teng, BB (2000). Hammerhead ribozyme as a therapeutic agent for hyperlipidemia: production of truncated apolipoprotein B and hypolipidemic effects in a dyslipidemia murine model. *Hum Gene Ther* **11**: 2415–2430.
8. Wang, JP, Enjoji, M, Tiebel, M, Ochsner, S, Chan, L and Teng, BB (1999). Hammerhead ribozyme cleavage of apolipoprotein B mRNA generates a truncated protein. *J Biol Chem* **274**: 24161–24170.
9. Dutta, R, Singh, U, Li, TB, Fornage, M and Teng, BB (2003). Hepatic gene expression profiling reveals perturbed calcium signaling in a mouse model lacking both LDL receptor and Apobec1 genes. *Atherosclerosis* **169**: 51–62.
10. Mak, S, Sun, H, Acevedo, F, Shimmin, LC, Zhao, L, Teng, BB *et al.* (2010). Differential expression of genes in the calcium-signaling pathway underlies lesion development in the LDb mouse model of atherosclerosis. *Atherosclerosis* **213**: 40–51.
11. Singh, U, Zhong, S, Xiong, M, Li, TB, Sniderman, A and Teng, BB (2004). Increased plasma non-esterified fatty acids and platelet-activating factor acetylhydrolase are associated with susceptibility to atherosclerosis in mice. *Clin Sci* **106**: 421–432.
12. Sun, H, Samarghandi, A, Zhang, N, Yao, Z, Xiong, M and Teng, BB (2012). Proprotein convertase subtilisin/kexin type 9 interacts with apolipoprotein B and prevents its intracellular degradation, irrespective of the low-density lipoprotein receptor. *Arterioscler Thromb Vasc Biol* **32**: 1585–1595.
13. Powell-Braxton, L, Véniant, M, Latvala, RD, Hirano, KI, Won, WB, Ross, J *et al.* (1998). A mouse model of human familial hypercholesterolemia: markedly elevated low density lipoprotein cholesterol levels and severe atherosclerosis on a low-fat chow diet. *Nat Med* **4**: 934–938.
14. Zhong, S, Sun, S and Teng, BB (2004). The recombinant adeno-associated virus vector (rAAV2)-mediated apolipoprotein B mRNA-specific hammerhead ribozyme: a self-complementary AAV2 vector improves the gene expression. *Genet Vaccines Ther* **2**: 5.
15. Chandak, PG, Obrowsky, S, Radovic, B, Doddapattar, P, Aflaki, E, Kratzer, A *et al.* (2011). Lack of acyl-CoA:diacylglycerol acyltransferase 1 reduces intestinal cholesterol absorption and attenuates atherosclerosis in apolipoprotein E knockout mice. *Biochim Biophys Acta* **1811**: 1011–1020.
16. Bowden, JA, Albert, CJ, Barnaby, OS and Ford, DA (2011). Analysis of cholesteryl esters and diacylglycerols using lithiated adducts and electrospray ionization-tandem mass spectrometry. *Anal Biochem* **417**: 202–210.
17. Rissanen, T, Voutilainen, S, Nyyssönen, K, Lakka, TA and Salonen, JT (2000). Fish oil-derived fatty acids, docosahexaenoic acid and docosapentaenoic acid, and the risk of acute coronary events: the Kuopio ischaemic heart disease risk factor study. *Circulation* **102**: 2677–2679.
18. Koliwad, SK, Streeper, RS, Monetti, M, Cornelissen, I, Chan, L, Terayama, K *et al.* (2010). DGAT1-dependent triacylglycerol storage by macrophages protects mice from diet-induced insulin resistance and inflammation. *J Clin Invest* **120**: 756–767.
19. Hansson, GK (2005). Inflammation, atherosclerosis, and coronary artery disease. *N Engl J Med* **352**: 1685–1695.
20. Fogelstrand, P and Borén, J (2012). Retention of atherogenic lipoproteins in the artery wall and its role in atherogenesis. *Nutr Metab Cardiovasc Dis* **22**: 1–7.
21. Sniderman, A, Couture, P and de Graaf, J (2010). Diagnosis and treatment of apolipoprotein B dyslipoproteinemias. *Nat Rev Endocrinol* **6**: 335–346.
22. Barter, PJ, Ballantyne, CM, Carmena, R, Castro Cabezas, M, Chapman, MJ, Couture, P *et al.* (2006). Apo B versus cholesterol in estimating cardiovascular risk and in guiding therapy: report of the thirty-person/ten-country panel. *J Intern Med* **259**: 247–258.
23. Di Angelantonio, E, Gao, P, Pennells, L, Kaptoge, S, Caslake, M, Thompson, A *et al.* (2012). Lipid-related markers and cardiovascular disease prediction. *Jama* **307**: 2499–2506.
24. Bell, DA, Hooper, AJ, Watts, GF and Burnett, JR (2012). Mipomersen and other therapies for the treatment of severe familial hypercholesterolemia. *Vasc Health Risk Manag* **8**: 651–659.
25. Visser, ME, Witztum, JL, Stroes, ES and Kastelein, JJ (2012). Antisense oligonucleotides for the treatment of dyslipidaemia. *Eur Heart J* **33**: 1451–1458.
26. Soutschek, J, Akinc, A, Bramlage, B, Charisse, K, Constien, R, Donoghue, M *et al.* (2004). Therapeutic silencing of an endogenous gene by systemic administration of modified siRNAs. *Nature* **432**: 173–178.
27. Koornneef, A, Maczuga, P, van Logtenstein, R, Borel, F, Blits, B, Ritsema, T *et al.* (2011). Apolipoprotein B knockdown by AAV-delivered shRNA lowers plasma cholesterol in mice. *Mol Ther* **19**: 731–740.
28. Maczuga, P, Lubelski, J, van Logtenstein, R, Borel, F, Blits, B, Fakkert, E *et al.* (2013). Embedding siRNA sequences targeting apolipoprotein B100 in shRNA and miRNA scaffolds results in differential processing and *in vivo* efficacy. *Mol Ther* **21**: 217–227.
29. Tadin-Strapps, M, Peterson, LB, Cumiskey, AM, Rosa, RL, Mendoza, VH, Castro-Perez, J *et al.* (2011). siRNA-induced liver ApoB knockdown lowers serum LDL-cholesterol in a mouse model with human-like serum lipids. *J Lipid Res* **52**: 1084–1097.
30. Kitajima, K, Marchadier, DH, Miller, GC, Gao, GP, Wilson, JM and Rader, DJ (2006). Complete prevention of atherosclerosis in apoE-deficient mice by hepatic human apoE gene transfer with adeno-associated virus serotypes 7 and 8. *Arterioscler Thromb Vasc Biol* **26**: 1852–1857.
31. Wang, L, Calcedo, R, Nichols, TC, Bellinger, DA, Dillow, A, Verma, IM *et al.* (2005). Sustained correction of disease in naive and AAV2-pretreated hemophilia B dogs: AAV2/8-mediated, liver-directed gene therapy. *Blood* **105**: 3079–3086.
32. Wang, L, Wang, H, Bell, P, McCarter, RJ, He, J, Calcedo, R *et al.* (2010). Systematic evaluation of AAV vectors for liver directed gene transfer in murine models. *Mol Ther* **18**: 118–125.
33. Yen, CL, Monetti, M, Burri, BJ and Farese, RV Jr (2005). The triacylglycerol synthesis enzyme DGAT1 also catalyzes the synthesis of diacylglycerols, waxes, and retinyl esters. *J Lipid Res* **46**: 1502–1511.
34. Cao, J, Zhou, Y, Peng, H, Huang, X, Stahler, S, Suri, V *et al.* (2011). Targeting Acyl-CoA:diacylglycerol acyltransferase 1 (DGAT1) with small molecule inhibitors for the treatment of metabolic diseases. *J Biol Chem* **286**: 41838–41851.
35. Yamamoto, T, Yamaguchi, H, Miki, H, Shimada, M, Nakada, Y, Ogino, M *et al.* (2010). Coenzyme A: diacylglycerol acyltransferase 1 inhibitor ameliorates obesity, liver steatosis, and lipid metabolism abnormality in KKAy mice fed high-fat or high-carbohydrate diets. *Eur J Pharmacol* **640**: 243–249.

36. Wochner, A, Attwater, J, Coulson, A and Holliger, P (2011). Ribozyme-catalyzed transcription of an active ribozyme. *Science* **332**: 209–212.

37. Knott, TJ, Wallis, SC, Powell, LM, Pease, RJ, Lusis, AJ, Blackhart, B *et al.* (1986). Complete cDNA and derived protein sequence of human apolipoprotein B-100. *Nucleic Acids Res* **14**: 7501–7503.

38. Sambrook, J and Russel, DW (2001). Rapid amplification of 5' cDNA ends (5'-Race). In: Irwin, N (ed.). *Molecular Cloning: A Laboratory Manual*, 3rd edn. Cold Spring Harbor Laboratory Press: Cold Spring Harbor, New York. pp. 8.54.

39. Teng, B, Blumenthal, S, Forte, T, Navaratnam, N, Scott, J, Gotto, AM Jr *et al.* (1994). Adenovirus-mediated gene transfer of rat apolipoprotein B mRNA-editing protein in mice virtually eliminates apolipoprotein B-100 and normal low density lipoprotein production. *J Biol Chem* **269**: 29395–29404.

40. Bligh, EG and Dyer, WJ (1959). A rapid method of total lipid extraction and purification. *Can J Biochem Physiol* **37**: 911–917.